International Journal of Pharmaceutics 391 (2010) 48–54

Contents lists available at ScienceDirect

International Journal of Pharmaceutics

journal homepage: www.elsevier.com/locate/ijpharm

Physical instability, aggregation and conformational changes of recombinant human bone morphogenetic protein-2 (rhBMP-2)

Ludmila Luca[a], Martinus A.H. Capelle[b], Gia Machaidze[c], Tudor Arvinte[a,b,*], Olivier Jordan[a], Robert Gurny[a]

[a] Department of Pharmaceutics and Biopharmaceutics, School of Pharmaceutical Sciences, University of Geneva, University of Lausanne, CH-1211 Geneva 4, Switzerland
[b] Therapeomic Inc., c/o University of Geneva, Department of Pharmaceutics and Biopharmaceutics, CH-1211 Geneva 4, Switzerland
[c] M.E. Mueller Institute of Structural Biology, Biozentrum, University of Basel, Basel, Switzerland

ARTICLE INFO

Article history:
Received 22 December 2009
Received in revised form 5 February 2010
Accepted 9 February 2010
Available online 13 February 2010

Keywords:
BMP-2
Aggregation
Physical stability
Fluorescence spectroscopy
Nile Red
1,8-ANS
Light scattering
Electron microscopy

ABSTRACT

The influence of two different pH values on the physical stability of recombinant human bone morphogenetic protein-2 (rhBMP-2) in aqueous solution was evaluated in the present work. RhBMP-2 in solution at pH 4.5 or 6.5 was characterized by intrinsic and extrinsic (Nile Red and 1,8-ANS) fluorescence spectroscopy, 90° light-scattering and transmission electron microscopy (TEM). Compared to the pH 4.5 solution, rhBMP-2 at pH 6.5 had (i) a stronger intrinsic fluorescence intensity, (ii) a longer fluorescence lifetime, (iii) a stronger 90° light-scattering intensity, (iv) a stronger Nile Red fluorescence intensity, (v) a higher Nile Red fluorescence anisotropy, (vi) a lower 1,8-ANS fluorescence intensity, (vii) a higher 1,8-ANS fluorescence anisotropy and (viii) a longer 1,8-ANS fluorescence lifetime. Electron microscopy showed that rhBMP-2 at pH 4.5 contained aggregates of about 100 nm in diameter. More and larger protein aggregates (0.1–2 μm) were observed in solution at pH 6.5. Taken together, these results indicate conformational changes and increased aggregation of rhBMP-2 at pH 6.5 compared to pH 4.5, demonstrating a strong influence of pH on rhBMP-2 physical stability. These observations must be considered when developing a delivery system for rhBMP-2.

1. Introduction

Discovered by M.R. Urist in 1965, bone morphogenetic protein-2 (BMP-2) is an important growth factor in bone formation and healing. BMP-2 belongs to the transforming growth factor-β (TGF-β) family, which are multifunctional cytokines that control cell proliferation and differentiation (Celeste et al., 1990). Considering the short half-life of the protein (Hsu et al., 2006; Senta et al., 2009), therapeutic applications of BMP-2 may benefit from a localized delivery system. To be clinically effective, a delivery system should retain BMP-2 at the implantation site for a sufficient time period and sufficient level (Li and Wozney, 2001).

In 2002, the first product containing recombinant human BMP-2 (rhBMP-2) was approved by the Food and Drug Administration (FDA) as an autograft replacement for interbody spinal fusion procedures and by the European Medicines Agency (EMEA) for the treatment of open tibial fractures (Geiger et al., 2003; McKay et al., 2007). To date, FDA and EMEA have approved both indications. The product is marketed as the INFUSE® Bone Graft kit (Medtronic) in the U.S. and as the InductOS® kit (Wyeth) in Europe and consists of lyophilized rhBMP-2 and an absorbable collagen sponge (ACS) carrier for the protein. The collagen sponge retains only a small amount of rhBMP-2 at the repair site (Uludag et al., 1999; Geiger et al., 2003), therefore the applied protein concentration (milligram range) is much higher than the physiologic concentration (nanogram range). To increase the retention of the protein at the implantation site, new types of delivery systems aiming at immobilization of growth factor have been investigated (Luginbuehl et al., 2004).

In order to preserve protein biological activity, particular attention should be given to the design of such a delivery system. Parameters like formulation pH, temperature conditions and shear stress can induce structural changes in proteins during manufacturing, storage, reconstitution and administration processes (Wang, 1999). One of the most common processes that may compromise the stability as well as the desired biological activity of protein drugs is the aggregation of individual molecules, which might lead ultimately to their precipitation (Manning et al., 1989; Middaugh and Volkin, 1992). Aggregates may also trigger other receptors which can result in undesired biological activity, side effects and toxicity (Bucciantini et al., 2002).

The pH of the formulation has a strong influence on the protein aggregation process. A change in pH will change the net charge of

* Corresponding author at: Department of Pharmaceutics and Biopharmaceutics, School of Pharmaceutical Sciences, University of Geneva, University of Lausanne, CH-1211 Geneva 4, Switzerland. Tel.: +41 22 379 63 39; fax: +41 22 379 65 67.
E-mail address: Tudor.Arvinte@unige.ch (T. Arvinte).

0378-5173/$ – see front matter © 2010 Elsevier B.V. All rights reserved.
doi:10.1016/j.ijpharm.2010.02.015

a protein and thus the balance between attractive and repulsive forces of protein molecules (Chi et al., 2003). At pH values close to the isoelectric point (pI), the relative contribution of attractive interactions between protein molecules increases, favoring precipitation. Regarding rhBMP-2 which pI is 8.2, the literature shows a reduced solubility at pH above 6 (Ruppert et al., 1996; Vallejo and Rinas, 2004). To ensure an adequate solubility, the commercially available rhBMP-2 is formulated in a 5 mM glutamic acid buffer pH 4.5 (Friess et al., 1999a; Schwartz, 2005). However, the combination of rhBMP-2 formulation at pH 4.5 with a delivery system may result in a pH shift toward higher pH. This was observed for instance with collagen sponge (ACS) (Friess et al., 1999a,b) as well as with other delivery systems (Maus et al., 2008; Bergman et al., 2008). An increase in pH might affect the stability of the protein which could influence the bioactivity of the system.

To our knowledge, no information is currently available on pH-dependent physical stability of rhBMP-2. This study investigates the influence of the formulation pH on the aggregation state and conformational changes of rhBMP-2. A commercial formulation of rhBMP-2 at pH 4.5 (InductOs®, Wyeth Pharmaceuticals) was used as a reference and compared with the same formulation neutralized to pH 6.5. This latter pH is close to the pH of the system currently used in clinic after combination of protein formulation with a collagen delivery carrier (Friess et al., 1999a). Various complementary methods, such as intrinsic and extrinsic (hydrophobic dyes Nile Red and 1,8-ANS) fluorescence spectroscopy, light scattering and transmission electron microscopy (TEM) were used to compare rhBMP-2 solutions at pH 4.5 and 6.5. These analytical techniques are well established for the characterization of chemical and physical stability of protein formulations (Pellaud et al., 1999; Lakowicz, 2004; Capelle et al., 2005; Jiskoot and Crommelin, 2005; Demeule et al., 2007b; Hawe et al., 2008).

2. Materials and methods

2.1. Materials

Lyophilized rhBMP-2 from the InductOs® kit (Wyeth Pharmaceuticals, Zug, Switzerland) was stored at −20 °C until use. This lyophilized formulation is composed of rhBMP-2 with 0.5% sucrose, 2.5% glycine, 5 mM L-glutamic acid, 5 mM sodium chloride and 0.01% polysorbate 80 (Friess et al., 1999b; Schwartz, 2005). The solution of rhBMP-2 at pH 4.5 was obtained by reconstitution of the lyophilizate with water. The solution of rhBMP-2 at pH 6.5 was obtained by adding the required quantity of 150 mM sodium hydroxide solution to the pH 4.5 solution. The pH was measured using a Biotrode glass electrode and a pH-meter from Metrohm (Herisau, Switzerland). The concentration of rhBMP-2 at both pH values was 0.75 mg/mL as determined by UV–visible absorbance. Nile Red (9-diethylamino-5*H*-benzo[α]phenoxazine-5-one) and 1,8-ANS (1-anilinonaphtalene-8-sulfonic acid) were purchased from Invitrogen (Luzern, Switzerland). Nile Red was dissolved in ethanol to produce a 100 μM stock solution, which was stored at 4 °C, protected from light. A stock solution of 5.35 mM 1,8-ANS in ethanol was prepared and stored at 4 °C, protected from light. Sucrose, glycine, glutamic acid, sodium chloride, polysorbate 80 and sodium hydroxide were purchased from Fluka (Buchs, Switzerland).

2.2. Steady-state fluorescence spectroscopy

The steady-state fluorescence and steady-state fluorescence anisotropy measurements were recorded with a Fluoromax spectrofluorometer (Spex, Stanmore, UK) at 25 °C in a thermostated cuvette holder. The measurements were performed in a 0.2 cm × 1 cm Hellma quartz cuvette with 400 μL of sample. For all fluorescence measurements, the large side of the cuvette (1 cm) was oriented towards the excitation beam. The intrinsic protein fluorescence, which is essentially due to the tryptophan residues, was monitored between 300 and 450 nm with an excitation wavelength of 280 nm. The spectra were recorded with 0.1 s integration time per 1 nm increment. The excitation and emission slits were set to 0.3 mm and 0.5 mm, respectively. The variation of the fluorescence between two samples of the same protein solution was less than 1%.

Nile Red fluorescence was monitored between 560 and 750 nm, with an excitation wavelength of 550 nm. The spectra were recorded with 0.1 s integration time per 1 nm increment. The excitation and emission slits were set to 1 mm and 2 mm, respectively. Prior to measurement, 4 μL of the Nile Red stock solution was added to 400 μL of the protein solution. 1,8-ANS fluorescence was monitored between 390 and 650 nm, with an excitation wavelength of 372 nm. The spectra were recorded with 0.01 s integration time per 1 nm increment. The excitation and emission slits were set to 0.5 mm and 1 mm, respectively. Prior to measurement 3.9 μL of the 1,8-ANS stock solution was added to 400 μL of the protein solution.

Steady-state fluorescence anisotropy measurements were performed using Glan-Thompson prism polarizers and the anisotropy A was calculated from the equation:

$$A = \frac{I_{0,0} - G \cdot I_{0,90}}{I_{0,0} + 2G \cdot I_{0,90}} \quad (1)$$

where $I_{m,n}$ is the fluorescence intensity at a given wavelength and the subscripts indicate the position of the polarizers in the excitation (m) and emission (n) beams relative to the vertical axis. G is a correction factor: $G = I_{90,0}/I_{90,90}$.

The anisotropy value of the protein fluorescence was calculated from fluorescence spectra between 335 and 360 nm, using an excitation wavelength of 280 nm, with 1 s integration time per 1 nm increment. The excitation and emission slits were both set to 3 mm.

The anisotropy value of the Nile Red fluorescence was calculated from fluorescence spectra between 610 and 640 nm, using an excitation wavelength of 550 nm, with 1 s integration time per 1 nm increment. The excitation and emission slits were set to 2 mm and 4 mm, respectively.

The fluorescence anisotropy value of 1,8-ANS was calculated from fluorescence spectra between 465 and 500 nm, using an excitation wavelength of 372 nm, with a 1 s integration time per 1 nm increment. The excitation and emission slits were set to 1 mm and 2 mm, respectively.

2.3. Steady-state fluorescence lifetime

Fluorescence lifetimes were measured using time-correlated single-photon counting (TCSPC) on an IBH 5000U fluorescence lifetime spectrophotometer (Jobin Yvon Horiba, New Jersey, USA). NanoLED sources with excitation wavelengths at 279 nm, 371 nm and 560 nm were used to measure the fluorescence lifetimes of protein, Nile Red and 1,8-ANS, respectively. The emitted photons were counted at 345 nm, 625 nm and 480 nm for protein, Nile Red and 1,8-ANS, respectively. For all lifetime measurements, the small side of the cuvette (0.2 cm) was oriented towards the excitation beam. Data analysis was performed using the DAS6 program (Jobin Yvon Horiba, New Jersey, USA). The measured fluorescence intensity decay was deconvoluted with the instrument response function, as measured using a dilute suspension of colloidal silica (Ludox, Aldrich, Milwaukee, USA). The calculated fluorescence intensity decay with time was fitted with a multi-exponential model. The intensity-weighted average fluorescence lifetime, τ_F, was calculated from the individual fluorescence decay times τ and the normalized pre-exponential values α using the equation

(Lakowicz, 2004):

$$\tau_F = \frac{\sum_{i=1}^{n} \alpha_i \tau_i^2}{\sum_{i=1}^{n} \alpha_i \tau_i} \quad (2)$$

where $n = 2$ or 3.

2.4. 90° static light scattering

The 90° static light scattering was measured with a Fluoromax spectrofluorometer (Spex, Stanmore, UK) at 25 °C in a thermostated cuvette holder. The measurements were performed in a 0.2 cm × 1 cm Hellma quartz cuvette with 400 μL of sample.

The measurement range was between 400 and 750 nm, with the excitation and emission monochromators synchronized. The spectra were recorded with a 0.01 s integration time per 1 nm increment. The excitation and emission slits were set to 0.5 mm and 1 mm, respectively. For light scattering measurements, the large side of the cuvette (1 cm) was oriented towards the excitation beam.

2.5. Transmission electron microscopy (TEM)

A 5-μL aliquot of the sample was incubated for 45 s on a freshly glow-discharged copper grid (200 mesh) covered with a parlodium/carbon film. The grid was sequentially washed with three drops of deionized water and stained for 45 s with 2% (w/v) freshly diluted and filtered uranyl acetate. Excess stain on the grid was absorbed by filter paper and the grid was subsequently air-dried; two grids were prepared per sample. The grids were analyzed using a Hitachi 7000 (Tokyo, Japan) transmission electron microscope with an acceleration voltage of 80 kV.

3. Results

3.1. Characterization of rhBMP-2 at two different pH values by steady-state fluorescence spectroscopy

RhBMP-2 was characterized by fluorescence spectroscopy at pH 4.5 and at pH 6.5 by intrinsic protein fluorescence as well as with the extrinsic fluorescent probes Nile Red and 1,8-ANS. The relative differences in fluorescence intensity, anisotropy, lifetime and calculated rotational correlation time of rhBMP-2 with and without fluorescent probes are summarized in Table 1. Absolute fluorescence parameters of rhBMP-2, Nile Red with rhBMP-2 and 1,8-ANS with rhBMP-2 are presented in Tables 2–4, respectively. At both pH values, the rhBMP-2 concentration was 0.75 mg/mL, as determined by UV–visible absorbance. The tryptophan fluorescence emission maxima for rhBMP-2 at pH 4.5 and pH 6.5 were 342 nm and 340 nm, respectively (Fig. 1). This 2-nm blue shift of the tryptophan fluorescence emission maximum, in addition to the 33% fluorescence intensity increase (Table 2), indicated a more hydrophobic environment for the tryptophan residues in the protein at pH 6.5, likely related to protein aggregation and conformational changes.

The extrinsic fluorescent dyes Nile Red and 1,8-ANS are used to detect changes in the tertiary structure of proteins (Hawe et al., 2008). The fluorescence intensity of 1 μM Nile Red with rhBMP-2 at pH 6.5 was about 39% stronger (Table 3) than at pH 4.5 (Fig. 2). Stronger fluorescence intensity is related to the increased binding of Nile Red to rhBMP-2 aggregates at pH 6.5. No difference was observed in the fluorescence intensity of Nile Red with rhBMP-2 at pH 4.5 and with the buffer formulation containing 0.005% polysorbate 80 (Fig. 2). Thus, at pH 4.5 the fluorescence emission of Nile Red with rhBMP-2 was in large part due to the fluorescence of Nile Red bound to the micelles of polysorbate 80.

Table 1
Relative differences [%] of steady-state fluorescence spectroscopy of rhBMP-2 and of extrinsic dyes with rhBMP-2 at pH 4.5 and at pH 6.5 are given. All parameters were normalized for rhBMP-2 formulation at pH 4.5. Absolute fluorescence parameters of rhBMP-2, Nile Red with rhBMP-2 and 1,8-ANS with rhBMP-2 are presented in Tables 2–4, respectively.

	I_{max}[a]	A[b]	τ_F[c]	τ_c[d]
rhBMP-2	+33	+5	+32	+50
1 μM Nile Red with rhBMP-2	+39	+19	−3	+25
50 μM 1,8-ANS with rhBMP-2	−19	+8	+8	+29

[a] Relative steady-state fluorescence intensity at the emission maximum.
[b] Relative steady-state fluorescence anisotropy.
[c] Relative intensity-weighted average fluorescence lifetime.
[d] Relative rotational correlation time.

Table 2
Fluorescence parameters of rhBMP-2 at pH 4.5 and pH 6.5.

	λ_{em}max[a] (nm)	I_{max}[b]	A[c]	τ_1[d] (ns)	α_1 (%)	τ_2 (ns)	α_2 (%)	τ_3 (ns)	α_3 (%)	τ_F[e] (ns)	Chi. Sq.[f]	τ_c[g] (ns)
rhBMP-2 pH 4.5	342	100	0.056	0.6	39.5	1.7	43.8	4.6	16.7	2.8	1.06	0.6
rhBMP-2 pH 6.5	340	133	0.059	0.6	28.8	1.9	44.2	5.2	27.0	3.7	1.21	0.9

[a] The steady-state fluorescence emission maximum.
[b] Relative steady-state fluorescence intensity at the emission maximum.
[c] The steady-state fluorescence anisotropy measured at 347 nm.
[d] The best fit to fluorescence lifetimes was obtained using three exponential terms: $I(\lambda, t) = \alpha_1(\lambda)\exp(-t/\tau_1) + \alpha_2(\lambda)\exp(-t/\tau_2) + \alpha_3(\lambda)\exp(-t/\tau_3)$, where τ_1, τ_2 and τ_3 are the decay times of the three components, and $\alpha_1(\lambda)$, $\alpha_2(\lambda)$ and $\alpha_3(\lambda)$ are the exponential factors at the emission wavelength λ.
[e] The intensity-weighted average fluorescence lifetime (see Section 2).
[f] Chi Square value reflects the quality of the mathematical fit: 1 is the best fit.
[g] The rotational correlation time (see Section 3).

Table 3
Fluorescence parameters of 1 μM Nile Red with rhBMP-2 at pH 4.5 and pH 6.5.

	λ_{em}max[a] (nm)	I_{max}[b]	A[c]	τ_1[d] (ns)	α_1 (%)	τ_2 (ns)	α_2 (%)	τ_F[e] (ns)	Chi. Sq.[f]	τ_c[g] (ns)
NR with rhBMP-2 at pH 4.5	625	100	0.127	0.9	10.4	3.5	89.6	3.4	1.18	1.6
NR with rhBMP-2 at pH 6.5	625	139	0.151	0.9	15.2	3.5	84.8	3.3	1.02	2.0

[a] The steady-state fluorescence emission maximum.
[b] Relative steady-state fluorescence intensity at the emission maximum.
[c] The steady-state fluorescence anisotropy measured at 625 nm.
[d] The best fit to fluorescence lifetimes was obtained using two exponential terms: $I(\lambda, t) = \alpha_1(\lambda)\exp(-t/\tau_1) + \alpha_2(\lambda)\exp(-t/\tau_2)$, where τ_1 and τ_2 are the decay times of the three components, and $\alpha_1(\lambda)$ and $\alpha_2(\lambda)$are the exponential factors at the emission wavelength λ.
[e] The intensity-weighted average fluorescence lifetime (see Section 2).
[f] Chi Square value reflects the quality of the mathematical fit: 1 is the best fit.
[g] The rotational correlation time (see Section 3).

Table 4
Fluorescence parameters of 50 μM 1,8-ANS with rhBMP-2 at pH 4.5 and pH 6.5.

	λ_{em}max[a] (nm)	I_{max}[b]	A[c]	τ_1[d] (ns)	α_1 (%)	τ_2 (ns)	α_2 (%)	τ_3 (ns)	α_3 (%)	τ_F[e] (ns)	Chi. Sq.[f]	τ_c[g] (ns)
1,8-ANS with rhBMP-2 at pH 4.5	480	100	0.213	0.9	5.1	5.5	40.1	13.7	54.8	11.7	1.24	13.4
1,8-ANS with rhBMP-2 at pH 6.5	480	81	0.231	0.7	5.0	5.9	43.2	14.9	51.8	12.6	1.07	17.3

[a] The steady-state fluorescence emission maximum.
[b] Relative steady-state fluorescence intensity at the emission maximum.
[c] The steady-state fluorescence anisotropy measured at 482 nm.
[d] The best fit to fluorescence lifetimes was obtained using three exponential terms: $I(\lambda, t) = \alpha_1(\lambda)\exp(-t/\tau_1) + \alpha_2(\lambda)\exp(-t/\tau_2) + \alpha_3(\lambda)\exp(-t/\tau_3)$, where τ_1, τ_2 and τ_3 are the decay times of the three components, and $\alpha_1(\lambda)$, $\alpha_2(\lambda)$ and $\alpha_3(\lambda)$ are the exponential factors at the emission wavelength λ.
[e] The intensity-weighted average fluorescence lifetime (see Section 2).
[f] Chi Square value reflects the quality of the mathematical fit: 1 is the best fit.
[g] The rotational correlation time (see Section 3).

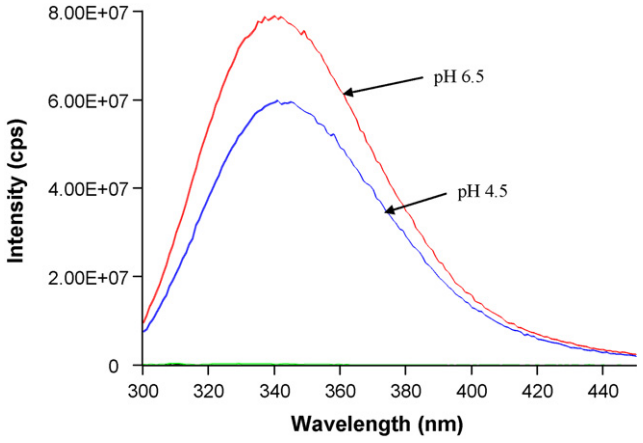

Fig. 1. Steady-state fluorescence emission spectra of rhBMP-2 at two different pH values.

A 19% decrease in fluorescence intensity was observed for 50 μM 1,8-ANS with rhBMP-2 at pH 6.5 compared to pH 4.5 (Table 4). The fluorescence intensity of 1,8-ANS with buffer formulation is lower compared to the fluorescence of 1,8-ANS with rhBMP-2 (Fig. 3). Our data show that the two dyes, 1,8-ANS and Nile Red, interact differently with the protein and its buffer. Nile Red binds predominantly to hydrophobic pockets of the rhBMP-2 aggregates and micelles of polysorbate 80. 1,8-ANS binds both via electrostatic and hydrophobic interactions to the positively charged protein (Matulis and Lovrien, 1998). Stronger fluorescence intensity of 1,8-ANS with rhBMP-2 at pH 4.5 compared to pH 6.5 is due to an increased binding of the dye to more positively charged protein molecules.

The intrinsic tryptophan fluorescence anisotropy slightly increased for rhBMP-2 at pH 6.5 compared to pH 4.5 (Table 2). The fluorescence anisotropy values of Nile Red with rhBMP-2 (Fig. 4) were 0.127 and 0.151 at pH 4.5 and pH 6.5, respectively, corresponding to a 19% increase (Table 3). The fluorescence anisotropy of 1,8-ANS with rhBMP-2 (Fig. 4) at pH 6.5 was higher than at pH 4.5 (Table 4). The fluorescence lifetime measurements showed three lifetime populations for the tryptophan in rhBMP-2 (Table 2) and for 1,8-ANS with protein (Table 4). Two lifetime populations were observed for Nile Red with rhBMP-2 (Table 3). As compared to rhBMP-2 at pH 4.5, the mean tryptophan fluorescence lifetime was about 32% longer for the pH 6.5 formulation. No significant difference in the mean fluorescence lifetime of Nile Red with rhBMP-2 at pH 4.5 and 6.5 was observed. The mean fluorescence lifetime of 1,8-ANS was longer with the protein at pH 6.5 than at pH 4.5. Higher fluorescence anisotropy and longer fluorescence lifetime indicated that the tryptophan residues in rhBMP-2 and extrinsic fluorescent dyes with rhBMP-2 were less mobile at pH 6.5 compared to pH 4.5. Decreased fluorophore molecular mobility indicates that it is located in a more hydrophobic environment, probably related to protein aggregation and conformational changes.

Steady-state fluorescence anisotropy A and the mean weighted fluorescence lifetime τ_F can be related to rotational diffusion of the fluorophore by the Perrin equation (Lakowicz, 2004):

$$\frac{A_0}{A} = 1 + \frac{\tau_F}{\tau_c} \quad (3)$$

where A_0 is the limit of fluorescence anisotropy and τ_c is the rotational correlation time. In turn, rotational correlation time is affected by the rapidity of the fluorophore reorientation and thus the molecular flexibility/rigidity of the protein or protein–dye complex. The rotational correlation time was calculated using the mean weighted fluorescence lifetime, fluorescence anisotropy and limit anisotropy values (A_0 is 0.3 for protein and 0.4 for dyes). Compared to the protein at pH 4.5, the rotational correlation time of

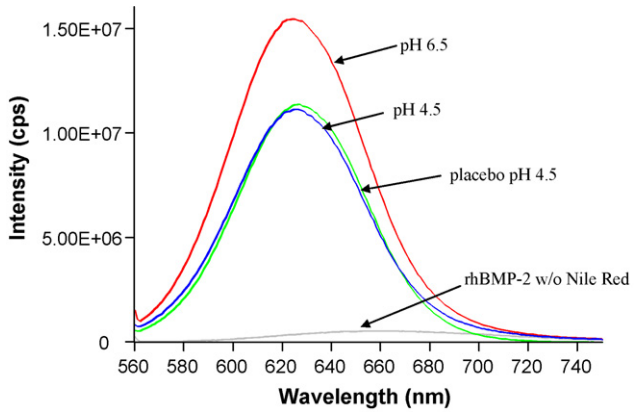

Fig. 2. Steady-state fluorescence emission spectra of 1 μM Nile Red with rhBMP-2 at two different pH values.

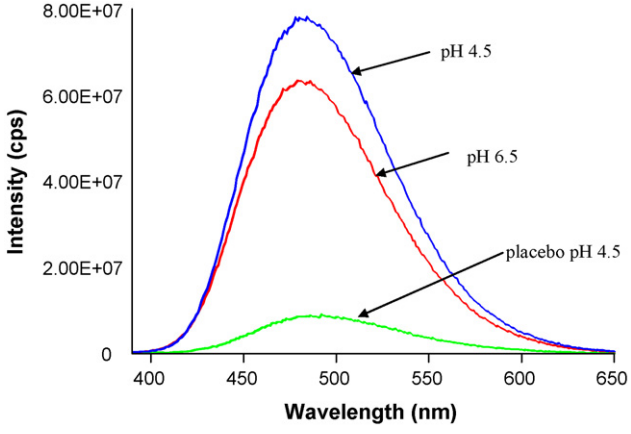

Fig. 3. Steady-state fluorescence emission spectra of 50 μM 1,8-ANS with rhBMP-2 at two different pH values.

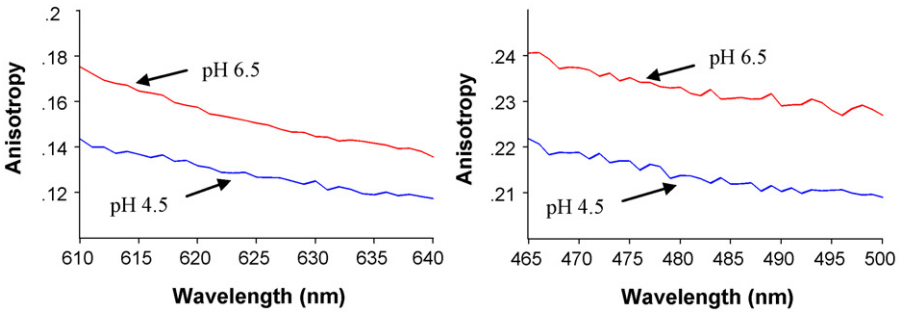

Fig. 4. Fluorescence anisotropy spectra of 1 μM Nile Red (left) and of 50 μM 1,8-ANS (right) with rhBMP-2 at two different pH values.

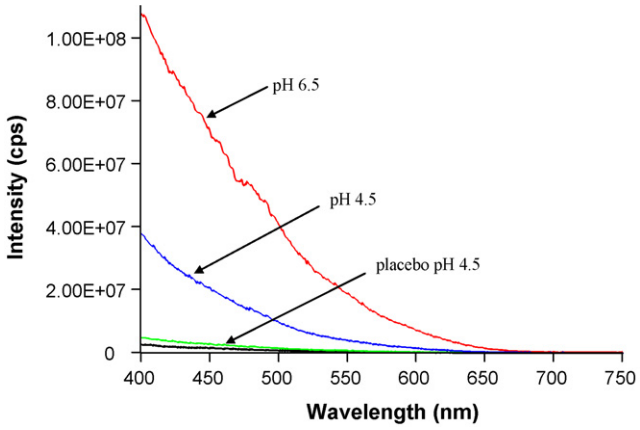

Fig. 5. 90° light-scattering spectra of rhBMP-2 at two different pH values.

tryptophan residues in the protein at pH 6.5 was about 50% longer (Table 2). At pH 6.5 the rotational correlation time of Nile Red with rhBMP-2 was about 25% longer than at pH 4.5 (Table 3). For 1,8-ANS with rhBMP-2 the rotational correlation time was 29% longer at pH 6.5 compared to pH 4.5 (Table 4). At pH 6.5, rhBMP-2 tryptophan residues and fluorescent dyes are located in a more hydrophobic environment compared to pH 4.5 as indicated by longer rotational correlation times.

3.2. 90° static light scattering

The 90° light scattering, monitored by running a synchronous scan ($\lambda_{exc} = \lambda_{em}$), was used to study protein aggregation. An approximately three-fold increase in light-scattering was observed for rhBMP-2 at pH 6.5 compared to the pH 4.5 formulation (Fig. 5).

3.3. Transmission electron microscopy (TEM)

RhBMP-2 solutions at pH 4.5 and 6.5 were observed by transmission electron microscopy (TEM). Immediately after reconstitution, both formulations contained protein aggregates. In solution at pH 4.5, protein aggregates of about 100 nm in diameter were visible only at higher magnification (Fig. 6C). In contrast, at pH 6.5, more and larger (0.1–2 μm in diameter) aggregates were observed in rhBMP-2 solution (Fig. 6B and D). Protein aggregates appeared amorphous in both formulations (Fig. 6). Electromicrographs of control buffer solutions (placebos) showed no particles (data not shown).

4. Discussion

The influence of two different pH values (4.5 and 6.5) on the physical stability of rhBMP-2 in solution was studied. Poor physical stability results from changes in the higher-order structure, including protein unfolding, aggregation, precipitation and adsorption to surfaces (Manning et al., 1989). The protein examined in this study is a human protein expressed in a genetically engineered Chinese hamster ovary (CHO) cell line. Following reconstitution with water of the rhBMP-2 lyophilizate containing buffer excipients, the pH of the formulation was 4.5. As seen by electron microscopy, the protein solution at pH 4.5 contained few amorphous aggregates (Fig. 6). In contrast, the aggregates at pH 6.5 were larger, different in shape and present in higher number compared to the aggregates in the formulation at pH 4.5 (Fig. 6). For both pH values no particles were detected in rhBMP-2 solution using Nile Red fluorescence microscopy. The Nile Red staining method was developed in our group to visualize protein aggregates with minimum size of 0.5 μm (Demeule et al., 2007a). This observation indicates the absence of rhBMP-2 aggregates larger than 0.5 μm in size at the two pH values. Aggregation of rhBMP-2 at pH 6.5 was confirmed by the observed three-fold increase in light scattering compared to pH 4.5. Protein aggregation is generally accompanied by modifications of molecular conformation (Chi et al., 2003). The enhanced, blue-shifted fluorescence intensity (Fig. 1) and longer fluorescence lifetime (Table 1) indicated a more hydrophobic environment for the tryptophan residues at pH 6.5 as a result of aggregation and conformational changes. According to the literature, the rhBMP-2 solution at pH 4.5 (2.5 mg/mL, Wyeth) contains about 1.2% of the protein as aggregates after reconstitution, as determined by size exclusion chromatography (SEC) (Schwartz, 2005). However, this analytical separation technique does not detect all types of aggregates (Philo, 2009). Loose aggregates, formed by weaker interactions, may be disrupted during the separation process, and their presence frequently remains undetected.

In addition, aggregation of rhBMP-2 accompanied by conformational changes was observed at pH 6.5 after protein staining with the extrinsic fluorescent dyes Nile Red and 1,8-ANS. In an aqueous environment, Nile Red and 1,8-ANS are essentially non-fluorescent and only become more fluorescent with increasing hydrophobicity of their environment (Sackett and Wolff, 1987; Matulis and Lovrien, 1998). Dyes can bind more efficiently to protein aggregates than to monomers due to the increased number of hydrophobic pockets. Changes in protein conformation, unfolding and chemical degradation are also detected by changes in the fluorescence properties of Nile Red or 1,8-ANS (Hawe et al., 2008). Nile Red is an uncharged, small hydrophobic fluorescent probe that binds predominantly via hydrophobic interactions and is therefore used for the study of protein degradation and aggregation (Sackett and Wolff, 1987; Demeule et al., 2007a). Nile Red fluorescence intensity has been shown to be unaffected by pH, at least between pH 4.5 and pH 8.5 (Sackett and Wolff, 1987; Capelle et al., 2009). In our study, the fluorescence of Nile Red with rhBMP-2 at pH 6.5 was stronger than with rhBMP-2 at pH 4.5 (Fig. 2). This increased fluorescence intensity was probably caused by the binding of Nile Red to the protein aggregates at pH 6.5. This hypothesis is strengthened

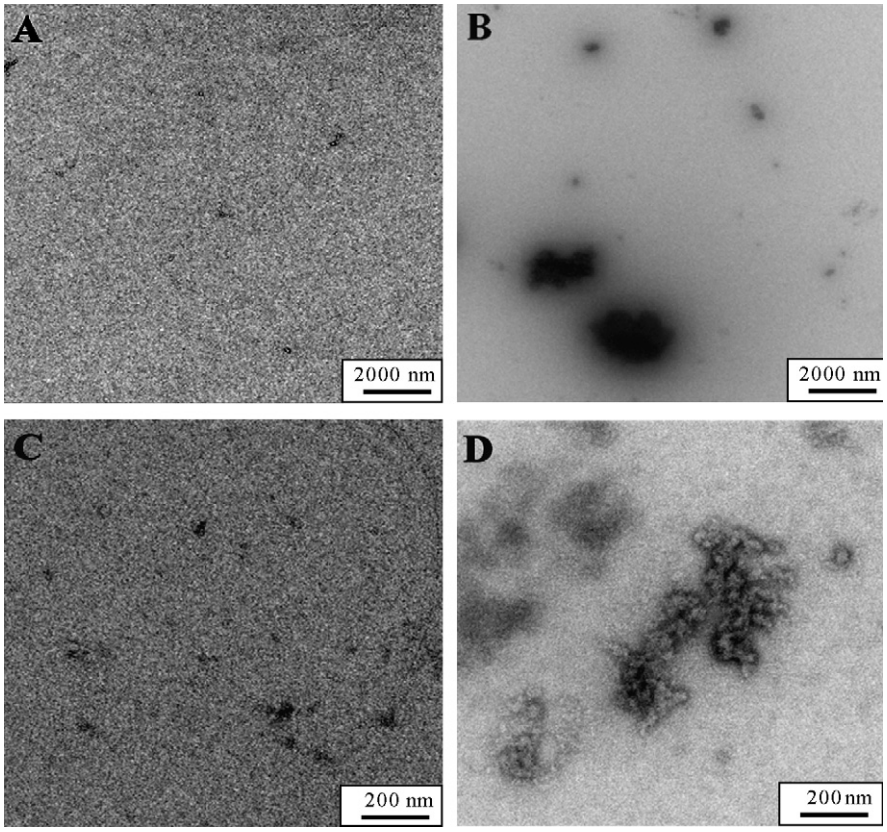

Fig. 6. Electron micrographs show amorphous aggregates of rhBMP-2 (0.75 mg/mL) at pH 4.5 (A; C) and pH 6.5 (B; D).

by the higher fluorescence anisotropy and longer rotational correlation time of Nile Red with rhBMP-2 at pH 6.5 compared to pH 4.5 (Table 1). This indicates that the bound Nile Red was located in a more hydrophobic environment at pH 6.5, which might be induced by conformational changes in the protein.

1,8-ANS binds primarily via electrostatic interactions to proteins (Matulis and Lovrien, 1998). At pH 4.5 and pH 6.5, 1,8-ANS contains negatively charged sulfonate groups and can bind to the positively charged areas of proteins (Matulis and Lovrien, 1998; Hawe et al., 2008). The – apparently contradictory – higher 1,8-ANS fluorescence intensity with rhBMP-2 at pH 4.5 compared to pH 6.5 (Fig. 3) was probably caused by an increase in the amount of electrostatically bound 1,8-ANS molecules as the protein is more positively charged (theoretical pI = 8.2) at pH 4.5 than at pH 6.5. The increase in 1,8-ANS fluorescence anisotropy and the increase in 1,8-ANS fluorescence lifetime (Table 1) both indicate that at pH 6.5, the binding of the dye to rhBMP-2 is stronger than at pH 4.5. The 1,8-ANS molecules bound to rhBMP-2 at pH 6.5 were less mobile than those bound to rhBMP-2 at pH 4.5. The calculated rotational correlation time of 1,8-ANS with rhBMP-2 at pH 6.5 was longer than at pH 4.5 (Table 1). The rotational correlation time indicated that 1,8-ANS bound to rhBMP-2 is in a more rigid environment at pH 6.5 as at pH 4.5. The 1,8-ANS fluorescence spectroscopy data indicate that rhBMP-2 exists in different conformation and aggregation state at the two pH values.

In the present study, we have shown that a shift of the pH of the rhBMP-2 formulation towards the physiological pH induces aggregation. This can be explained by a reduction of the electrostatic repulsive interactions when approaching the isoelectric point of 8.2, leading to an increase in the relative contribution of hydrophobic attractive interactions (Chi et al., 2003). The observed pH-induced conformational changes of rhBMP-2 probably led to the exposure of hydrophobic patches. The individual protein molecules have a tendency to aggregate in order to minimize the unfavorable interaction between hydrophobic residues and the hydrophilic solvent (Wang, 1999; Morris et al., 2009).

An important limitation for the use of proteins as therapeutic drugs is precipitation, which is the macroscopic equivalent of aggregation (Manning et al., 1989). As a consequence of conformational protein modifications, the precipitation process starts with the association of molecules dispersed in solution into primary particles that eventually flocculate to form a precipitate (Glatz, 1992). The reported pH-dependent rhBMP-2 solubility during production (Ruppert et al., 1996; Vallejo and Rinas, 2004) could thus be a consequence of pH-induced conformational changes in the protein that cause aggregation leading to precipitation.

Moreover, the fact that rhBMP-2 solubility increases in acidic environment is thought to be relevant for its pharmacological effect. Early in the bone-fracture response, the extracellular compartment between osteoclasts and bone matrix is acidified (pH 4–5). Osteoclasts secrete protons and enzymes into the extracellular environment (the bone-resorbing compartment) to allow the dissolution of the mineral constituents and digestion of organic components of the bone matrix (Baron et al., 1985; Silver et al., 1988; Hollinger and Wong, 1996). This acidified microenvironment in the extracellular compartment probably provides an optimal solubility, stability and bioactivity of BMP-2 at the site of tissue remodeling.

RhBMP-2 is not the only protein in the TGF-β family that shows pH-dependent aggregation. TGF-β3 forms large precipitating aggregates around physiological pH and conformational changes of the protein are associated with aggregation (Pellaud et al., 1999). In addition, similarly to rhBMP-2 (Koenig et al., 1994), TGF-β3 has a high tendency to adsorb onto hydrophobic surfaces.

The use of complementary analytical methods such as tryptophan-fluorescence spectroscopy, light scattering and trans-

mission electron microscopy allowed a reliable assessment of aggregation and alterations in the conformation of rhBMP-2 at pH 6.5. On the other hand, the extrinsic fluorescent dyes Nile Red and 1,8-ANS provided additional information about the pH effect on the conformation and aggregation state of rhBMP-2.

Taken together, these data indicate that the pH conditions of a delivery system for rhBMP-2 should be carefully considered in order to optimize protein stability for a therapeutic application. The observed pH-induced conformational changes and aggregation of rhBMP-2 are expected to impact protein biological activity. *In vivo* studies are needed to investigate the influence of protein conformational changes and aggregation on the biological activity.

References

Baron, R., Neff, L., Louvard, D., Courtoy, P.J., 1985. Cell-mediated extracellular acidification and bone resorption: evidence for a low pH in resorbing lacunae and localization of a 100-kD lysosomal membrane protein at the osteoclast ruffled border. J. Cell Biol. 101, 2210–2222.

Bergman, K., Engstrand, T., Hilborn, J., Ossipov, D., Piskounova, S., Bowden, T., 2008. Injectable cell-free template for bone-tissue formation. J. Biomed. Mater. Res. A 91, 1111–1118.

Bucciantini, M., Giannoni, E., Chiti, F., Baroni, F., Formigli, L., Zurdo, J., Taddei, N., Ramponi, G., Dobson, C.M., Stefani, M., 2002. Inherent toxicity of aggregates implies a common mechanism for protein misfolding diseases. Nature 416, 507–511.

Capelle, M.A., Brugger, P., Arvinte, T., 2005. Spectroscopic characterization of antibodies adsorbed to aluminium adjuvants: correlation with antibody vaccine immunogenicity. Vaccine 23, 1686–1694.

Capelle, M.A., Gurny, R., Arvinte, T., 2009. A high throughput protein formulation platform: case study of salmon calcitonin. Pharm. Res. 26, 118–128.

Celeste, A.J., Iannazzi, J.A., Taylor, R.C., Hewick, R.M., Rosen, V., Wang, E.A., Wozney, J.M., 1990. Identification of transforming growth factor beta family members present in bone-inductive protein purified from bovine bone. Proc. Natl. Acad. Sci. U.S.A. 87, 9843–9847.

Chi, E.Y., Krishnan, S., Randolph, T.W., Carpenter, J.F., 2003. Physical stability of proteins in aqueous solution: mechanism and driving forces in nonnative protein aggregation. Pharm. Res. 20, 1325–1336.

Demeule, B., Gurny, R., Arvinte, T., 2007a. Detection and characterization of protein aggregates by fluorescence microscopy. Int. J. Pharm. 329, 37–45.

Demeule, B., Lawrence, M.J., Drake, A.F., Gurny, R., Arvinte, T., 2007b. Characterization of protein aggregation: the case of a therapeutic immunoglobulin. Biochim. Biophys. Acta 1774, 146–153.

Friess, W., Uludag, H., Foskett, S., Biron, R., 1999a. Bone regeneration with recombinant human bone morphogenetic protein-2 (rhBMP-2) using absorbable collagen sponges (ACS): influence of processing on ACS characteristics and formulation. Pharm. Dev. Technol. 4, 387–396.

Friess, W., Uludag, H., Foskett, S., Biron, R., Sargeant, C., 1999b. Characterization of absorbable collagen sponges as rhBMP-2 carriers. Int. J. Pharm. 187, 91–99.

Geiger, M., Li, R.H., Friess, W., 2003. Collagen sponges for bone regeneration with rhBMP-2. Adv. Drug Deliv. Rev. 55, 1613–1629.

Glatz, C.E., 1992. Modeling of aggregation-precipitation phenomena. In: Ahern, T.J., Manning, M.C. (Eds.), Stability of Protein Pharmaceuticals, Part A: Chemical and Physical Pathways of Protein Degradation. Plenum Press, New York, pp. 135–166.

Hawe, A., Sutter, M., Jiskoot, W., 2008. Extrinsic fluorescent dyes as tools for protein characterization. Pharm. Res. 25, 1487–1499.

Hollinger, J., Wong, M.E., 1996. The integrated processes of hard tissue regeneration with special emphasis on fracture healing. Oral Surg. Oral Med. Oral Pathol. Oral Radiol. Endod. 82, 594–606.

Hsu, H.P., Zanella, J.M., Peckham, S.M., Spector, M., 2006. Comparing ectopic bone growth induced by rhBMP-2 on an absorbable collagen sponge in rat and rabbit models. J. Orthop. Res. 24, 1660–1669.

Jiskoot, W., Crommelin, D., 2005. Methods for Structural Analysis of Protein Pharmaceuticals. AAPS Press, Arlington.

Koenig, B.B., Cook, J.S., Wolsing, D.H., Ting, J., Tiesman, J.P., Correa, P.E., Olson, C.A., Pecquet, A.L., Ventura, F., Grant, R.A., 1994. Characterization and cloning of a receptor for BMP-2 and BMP-4 from NIH 3T3 cells. Mol. Cell. Biol. 14, 5961–5974.

Lakowicz, J.R., 2004. Principles of Fluorescence Spectroscopy, 2nd ed. Springer Science, New York.

Li, R.H., Wozney, J.M., 2001. Delivering on the promise of bone morphogenetic proteins. Trends Biotechnol. 19, 255–265.

Luginbuehl, V., Meinel, L., Merkle, H.P., Gander, B., 2004. Localized delivery of growth factors for bone repair. Eur. J. Pharm. Biopharm. 58, 197–208.

Manning, M.C., Patel, K., Borchardt, R.T., 1989. Stability of protein pharmaceuticals. Pharm. Res. 6, 903–918.

Matulis, D., Lovrien, R., 1998. 1-Anilino-8-naphthalene sulfonate anion-protein binding depends primarily on ion pair formation. Biophys. J. 74, 422–429.

Maus, U., Andereya, S., Gravius, S., Siebert, C.H., Ohnsorge, J.A., Niedhart, C., 2008. Lack of effect on bone healing of injectable BMP-2 augmented hyaluronic acid. Arch. Orthop. Trauma Surg. 128, 1461–1466.

McKay, W.F., Peckham, S.M., Badura, J.M., 2007. A comprehensive clinical review of recombinant human bone morphogenetic protein-2 (INFUSE Bone Graft). Int. Orthop. 31, 729–734.

Middaugh, C.R., Volkin, D.B., 1992. Protein solubility. In: Ahern, T.J., Manning, M.C. (Eds.), Stability of Protein Pharmaceuticals, Part A: Chemical and Physical Pathways of Protein Degradation. Plenum Press, New York, pp. 109–134.

Morris, A.M., Watzky, M.A., Finke, R.G., 2009. Protein aggregation kinetics, mechanism, and curve-fitting: a review of the literature. Biochim. Biophys. Acta 1794, 375–397.

Pellaud, J., Schote, U., Arvinte, T., Seelig, J., 1999. Conformation and self-association of human recombinant transforming growth factor-beta3 in aqueous solutions. J. Biol. Chem. 274, 7699–7704.

Philo, J.S., 2009. A critical review of methods for size characterization of non-particulate protein aggregates. Curr. Pharm. Biotechnol. 10, 359–372.

Ruppert, R., Hoffmann, E., Sebald, W., 1996. Human bone morphogenetic protein 2 contains a heparin-binding site which modifies its biological activity. Eur. J. Biochem. 237, 295–302.

Sackett, D.L., Wolff, J., 1987. Nile red as a polarity-sensitive fluorescent probe of hydrophobic protein surfaces. Anal. Biochem. 167, 228–234.

Schwartz, D., 2005. Development of an Aqueous Suspension of Recombinant Human Bone morphogenetic Protein-2 (rhBMP-2). Ph.D. Thesis, University of Munich, Germany.

Senta, H., Park, H., Bergeron, E., Drevelle, O., Fong, D., Leblanc, E., Cabana, F., Roux, S., Grenier, G., Faucheux, N., 2009. Cell responses to bone morphogenetic proteins and peptides derived from them: biomedical applications and limitations. Cytokine Growth Factor Rev. 20, 213–222.

Silver, I.A., Murrills, R.J., Etherington, D.J., 1988. Microelectrode studies on the acid microenvironment beneath adherent macrophages and osteoclasts. Exp. Cell Res. 175, 266–276.

Uludag, H., Friess, W., Williams, D., Porter, T., Timony, G., D'Augusta, D., Blake, C., Palmer, R., Biron, B., Wozney, J., 1999. rhBMP-collagen sponges as osteoinductive devices: effects of in vitro sponge characteristics and protein pI on in vivo rhBMP pharmacokinetics. Ann. N. Y. Acad. Sci. 875, 369–378.

Vallejo, L.F., Rinas, U., 2004. Optimized procedure for renaturation of recombinant human bone morphogenetic protein-2 at high protein concentration. Biotechnol. Bioeng. 85, 601–609.

Wang, W., 1999. Instability, stabilization, and formulation of liquid protein pharmaceuticals. Int. J. Pharm. 185, 129–188.